ON THE CONTROL CONSTRAINTS OF DC-DC BOOST CONVERTERS

Pagano, D. J. and Cunha, F. B.
Departamento de Automação e Sistemas,
Universidade Federal de Santa Catarina,
88040-900, Florianópolis, SC, Brasil
daniel@das.ufsc.br, felipe.cunha@braskem.com.br

Abstract— **In this paper, the control of DC-DC boost converters is analyzed using both instantaneous and averaged models. The control objectives are discussed and the main focus is the load disturbance rejection. The transient performance is shown to be limited by saturation constraints on the control variable. In particular, it is shown that the transient behaviour of the output voltage in the presence of load disturbances cannot be minimized beyond a certain limit by the control strategy. Constraints on the frequency spectra of the current signals are also commented. A comparative simulation study considering two different control laws put in evidence these limitations.**

KEYWORDS

Switching Systems, boost converters, constraints, sliding mode, washout filter.

I. INTRODUCTION

The DC-DC boost converter is an electronic system which transfers electric power from a voltage source to an output load. The main task of such a system is to provide a regulated output voltage greater than its input voltage. The boost performs this task by means of switching elements that govern the energy transfer from the input to the output. The circuit operation can be divided into two stages: (i) the energy accumulation in the input inductor, (ii) the energy transfer to the output capacitor. The design of this system comprises, among other things, choosing the best way to perform this energy transfer with minimum losses [1], [2].

Besides these efficiency issues, the boost output should be robust with respect to load changes and fluctuations of the input voltage source. While the efficiency is basically a *design problem*, the disturbance rejection is traditionally a *control problem*. This stated, the main objective in the boost converter control is, in the presence of such disturbances, to drive the output voltage back to its nominal value with a minimum transient behaviour.

This paper intents to show that the transient behaviour of the output voltage in the presence of load disturbances cannot be minimized beyond a certain limit by the control strategy. This limit arises from the inner structural characteristics of the boost converter and can only be minimized if the desired transient behaviour is taken into account in the design phase of this power electronic device.

II. DC-DC BOOST CONVERTER

A schematic representation of the basic DC-DC boost converter with ideal switching is given in Fig.1.

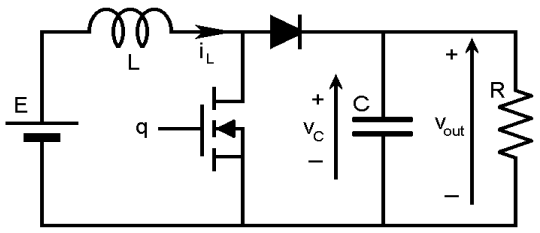

Fig. 1. DC-DC boost converter circuit.

The circuit analysis of the boost converter in Fig.1 operating in CCM leads to the nonlinear state space equation

$$\begin{cases} \dot{x}_1 = -\frac{1}{L}(1-q)x_2 + \frac{1}{L}E \\ \dot{x}_2 = \frac{1}{C}(1-q)x_1 - \frac{1}{RC}x_2 \end{cases} \quad (1)$$

where $x_1 = i_L$, $x_2 = v_C$ and q represents the discrete state of the switch.

Eq. (1) is known in the literature as the ideal *instantaneous model*, but it can also be seen as the *averaged model*. Under this point of view, the variables x_1 and x_2 are the time averages of the instantaneous values of i_L and v_C, respectively and the discrete instantaneous signal q can be substituted by the duty cycle d of a high frequency PWM control signal applied to the switch [3].

Each of these two approaches gives rise to different controller families: (i) those based on the instantaneous model and (ii) those based on the averaged model.

No matter how Eq.(1) is treated, the equilibrium points the boost can exhibit are the same. They can be calculated by imposing $\dot{x}_1 = 0$ and $\dot{x}_2 = 0$ and eliminating q from the resulting algebraic system. This procedure gives the following set of possible equilibria:

$$\Gamma = \left\{ (x_1, x_2) \in \mathbf{R}^2 \Big/ x_1 = \frac{{x_2}^2}{RE} \right\} \quad (2)$$

which is a 1-dimension manifold in the state space. All equilibrium points of (1) must lie on the manifold Γ regardless of the function q. When q is replaced by its average d each point in Γ corresponds to the equilibrium

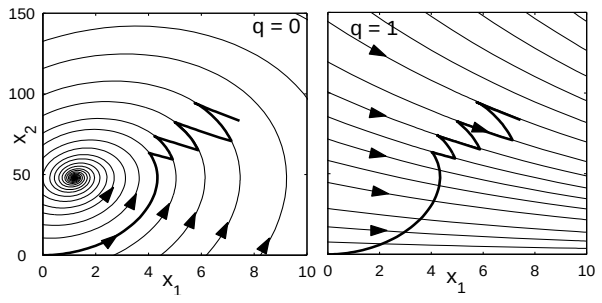

Fig. 2. Natural trajectories of the ideal boost model.

associated with a constant value $d = D$. These equilibria are given by

$$\overline{X}_1 = \frac{E}{R(1-D)^2}; \qquad \overline{X}_2 = \frac{E}{(1-D)}. \tag{3}$$

Note that the set Γ depends on the values of R and E.

A. Instantaneous Model

The controllers designed based on the instantaneous model generally act directly at the switch deciding when it is to be commuted.

To analyse the instantaneous model each operating stage has to be considered separately. When $q = 0$, Eq.(1) becomes

$$\begin{cases} \dot{x}_1 = -\frac{1}{L}x_2 + \frac{1}{L}E \\ \dot{x}_2 = \frac{1}{C}x_1 - \frac{1}{RC}x_2. \end{cases} \tag{4}$$

The dynamic system described by Eq. (4) will be referred to as the *0-structure* of the boost converter. This 0-structure exhibits a linear dynamic around the unique equilibrium point

$$\overline{X}_0 = \begin{bmatrix} \bar{x}_{0_1} \\ \bar{x}_{0_2} \end{bmatrix} = \begin{bmatrix} E/R \\ E \end{bmatrix}. \tag{5}$$

When $q = 1$ the system (1) reduces to

$$\begin{cases} \dot{x}_1 = \frac{1}{L}E \\ \dot{x}_2 = -\frac{1}{RC}x_2. \end{cases} \tag{6}$$

Eq.(6) will be referred to as the *1-structure* of the system (1). This structure has no equilibrium points and its analytic solution is

$$\begin{cases} x_1(t) = x_{1_0} + \frac{E}{L}t \\ x_2(t) = x_{2_0}e^{-\frac{t}{RC}}. \end{cases} \tag{7}$$

All possible trajectories of the system (1), in open or closed loop, are constructed with combinations of pieces of the *natural trajectories* given by the solutions of Eqs. (4) and (6). Fig. 2 shows an arbitrary trajectory as an exemple.

B. Averaged and Linearized Models

Another possible approach to the analysis of the boost converter is to consider Eq.(1) as the averaged model. In this case, the switch is operated by a PWM signal modulated by a continuous control variable d that takes the place of q in (1) and represents its duty cycle.

Continuous nonlinear control functions can be synthesized directly from the averaged nonlinear model [4], [5], [6] but the most traditional way to control the boost is to linearize Eq. (1) around the desired equilibrium point and to design a linear controller for the linearized system [7]. After expanding the righthand side of (1) in Taylor series and neglecting the nonlinear terms, the linearized model becomes

$$\begin{aligned} \begin{bmatrix} \dot{\tilde{x}}_1 \\ \dot{\tilde{x}}_2 \end{bmatrix} = & \begin{bmatrix} 0 & -\frac{(1-D)}{L} \\ \frac{(1-D)}{C} & -\frac{1}{RC} \end{bmatrix} \cdot \begin{bmatrix} \tilde{x}_1 \\ \tilde{x}_2 \end{bmatrix} \\ & + \begin{bmatrix} \frac{V_C}{L} \\ -\frac{I_L}{C} \end{bmatrix} \cdot \tilde{d} + \begin{bmatrix} \frac{1}{L} & 0 \\ 0 & \frac{V_C}{R^2C} \end{bmatrix} \cdot \begin{bmatrix} \tilde{e} \\ \tilde{r} \end{bmatrix} \end{aligned} \tag{8}$$

where $[I_L\ V_C]^T$ is the desired equilibrium point, D, R and E are the nominal duty cycle, load and voltage source, respectively. The control input is represented by $\tilde{d}$, and the disturbance variables $\tilde{e}$ and $\tilde{r}$ are fluctuations about the nominal values of E and R, respectively. Note that this linearized model is only valid in the neighborhood of the equilibrium point, around which the linearization was done. So, it only represents the system response to small perturbations of the input signals. If the state vector is far from the equilibrium point or if the disturbance range is wide, the linearized model loses its validity.

III. CONTROL OBJECTIVES AND CONSTRAINTS

The DC-DC boost converter must be insensitive with respect to load disturbances and fluctuations of the voltage source. This paper focuses on the load disturbance rejection problem from a geometric approach of the saturation constraint on the control variable d.

A. Constraint on the Control

As it is well known, every control is subject to some constraints. In the case of most power electronic converters, the only available control variables are the states of a certain number of switches. This means that the continuous output variables need to be controlled by discrete control variables: the state of the switches.

Under the assumption that the switch operates according to a high frequency PWM control signal, it is possible to replace the discrete control variable q by its duty cycle d. The control saturation is inherent to this procedure and the saturation limits correspond to the discrete states of the switch. For this reason, the duty cycle can only vary in the real interval [0, 1]. The examples shown in Fig.3 illustrate this effect. All trajectories start from the same initial condition and evolve according to a fixed duty cycle d. It is clear from Fig.3 that there is a certain zone below the trajectories with $d = 0$ and $d = 1$ which cannot be achieved directly.

If the control strategy does not make use of pulse width modulation, the discrete nature of the control input is itself the constraint on the control law, which can only decide if the input should be *switch on* or *switch off*.

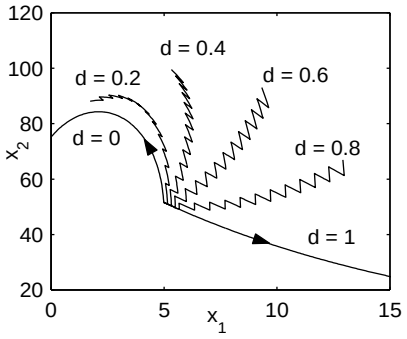

Fig. 3. Range of possible trajectories under different constant duty cycle subject to the saturation limits $d = 0$ and $d = 1$.

B. Constraint on the frequency spectra

Another important constraint in the control of power electronic devices are the frequency spectra of the current signals. If these signals have frequency components in the audible band of the spectrum, the inductors may vibrate producing audible noise. To overcome this drawback it is necessary that the switches operate in frequencies above the audible band. In addition, if using PWM, the control duty cycle cannot vary periodically in an audible frequency. If this occurs, despite of the high fixed frequency PWM, the periodic variation of the duty cycle produces oscillating currents in the inductors which may cause audible noise.

Beside these low frequency restrictions there is also a high frequency constraint. When using a PWM signal to implement the control the duty cycle must vary slowly compared to the PWM frequency, otherwise the pulse width modulator could not reproduce the duty cycle wave form in its output. Also, the PWM frequency has limitations caused by the heat generation in the switching elements.

C. Load Disturbance Rejection

To analyse the load disturbance rejection it is necessary to consider how a change in resistance affects the state space trajectories. As stated in Section II, the set Γ, loci of all possible equilibria, also changes under a load disturbance. This effect is shown in Fig.4.

Suppose that a boost converter is required to operate under a certain load range and that the load increases or decreases instantaneously by step changes. Under these hypotheses, the most critical case occurs when the load changes from its maximum value to its minimum and then returns to its maximum. To illustrate this idea, in this work, a $250W$ DC-DC boost with $C = 10\mu F$, $L = 1.4mH$, $E = 48V$ and $V_C = 100V$ operating at a $40kHz$ frequency is considered. The load range goes from 20% ($R = 200\Omega$) up to 100% ($R = 40\Omega$) of the nominal power. The equilibrium manifolds corresponding to these two extreme cases are represented as $\Gamma(R_{max})$ and $\Gamma(R_{nom})$ respectively in Fig. 4.

Consider the case where the boost is in steady state working with full load and the output resistance suddenly changes from $R_a = 40\Omega$ to $R_b = 200\Omega$. Thus, the control

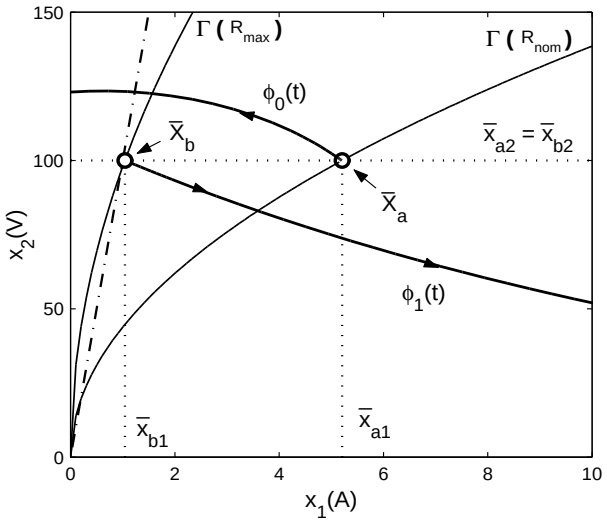

Fig. 4. System trajectories in the state space (x_1, x_2) for saturated duty cycle $d = 0$ ($\phi_0(t)$) and $d = 1$ ($\phi_1(t)$), considering $R_{nom} = 40\Omega$ and $R_{max} = 200\Omega$.

task is to drive the system state from $\overline{X}_a$ to $\overline{X}_b$ minimizing the undesirable transient effects. In other words, the current is required to decrease to $\bar{x}_{b_1}$ within minimum time and the voltage must settle in the desired regulated value $\bar{x}_{b_2} = V_C$ after going through a minimum overshoot also within minimum time.

In order to reach the new equilibrium point $\overline{X}_b$ in a short time it is necessary to decrease the inductor current as fast as possible. The only way to do so is to saturate the duty cycle in its minimum value, which means to leave the switch on the position $q = 0$. In this case, the state vector moves along the natural trajectory $\phi_0(t)$ (see Fig.4), that represents the behaviour of the system in a saturation condition of the control. This trajectory alone does not lead to the desired equilibrium point. It means that the duty cycle cannot remain in its saturation value. After evolving by ϕ_0 for some time, the state of the system has to be forced towards the desired equilibrium point $\overline{X}_b$. At this moment, the controller has to make the decision of changing the value of the duty cycle in order to lead the state vector toward the point $\overline{X}_b$.

Consider the region where the vertical component of the phase velocity vector is always greater for $q = 0$ than for $q = 1$. It can be shown from (1) that this region is the one that lies at the righthand side of the line given by

$$x_2 = \frac{R}{2} x_1 \tag{9}$$

represented as a dashed-dotted line in Fig.(4). The problem is that, if the the system starts to switch before reaching this line, the combination of trajectories from the two structures makes the overshoot to increase, as can be seen in Fig.(3). As the only possible trajectories are those composed by switching between the two structures of the system, to make the transition from $\overline{X}_a$ to $\overline{X}_b$ with minimum overshoot, the system has to leave saturation near the line given by (9).

In the neighborhood of Γ, the magnitude of the average phase velocity vector is small since Γ is the geometric place where the combination of the phase velocity vector of the two different structures becomes null. This causes the state vector to converge slowly to the new equilibrium point $\overline{X}_b$ if the system state is forced to evolve along a switching trajectory close to Γ. If the state vector is required to converge fast to the equilibrium point, the control has to drive the system through a trajectory far from the equilibrium manifold.

IV. COMPARATIVE STUDY OF TWO DIFFERENT CONTROLLERS

In this work, two different controllers are compared: (i) a classic linear PID controller and (ii) a sliding mode controller with a washout filter.

Consider first the linearized model (8). The transfer function from the duty cycle to the output voltage is

$$G(s) = -\frac{I_L}{C}\frac{s - \frac{R}{L}(1-D)^2}{s^2 + \frac{1}{RC}s + \frac{(1-D)^2}{LC}} \tag{10}$$

where $I_L = \frac{V_C^2}{RE}$ and the other parameters are defined in Subsection III-C.

In a previous work [8], a linear PID controller was designed by the rootlocus method for the linear model. The parameters obtained by this procedure were finely tuned via simulations of the closed loop nonlinear model leading to the following controller:

$$C(s) = 0.3\frac{s^2 + 3000s + 3534^2}{s(s + 2\times 10^5)}. \tag{11}$$

The performance of the linear PID controller is compared with the sliding mode controller combined with a washout filter developed in [9] (see also [10]). The washout filter consists of a high pass transfer function in the feedback loop of one or more state variables. For the boost converter, the filter is introduced in the current feedback. The reason for this is that the output voltage control should not depend on the value of the steady state current, but the load disturbance rejection dynamics can be optimized by considering the transient current.

The simplest washout filter is a first order high pass filter expressed by

$$H(s) = \frac{s}{s+\omega} \quad \text{with} \quad X_3(s) = H(s)X_1(s). \tag{12}$$

Note that x_3 is the output of the filter applied on x_1. The instantaneous model of the boost converter can be extended to include the dynamics of this filter, which leads to the state space equation

$$\begin{bmatrix} \dot{x}_1 \\ \dot{x}_2 \\ \dot{x}_3 \end{bmatrix} = \begin{bmatrix} \frac{E}{L} \\ -\frac{x_2}{RC} \\ \frac{E}{L} - \omega x_3 \end{bmatrix} + \begin{bmatrix} -\frac{x_2}{L} \\ \frac{x_1}{C} \\ -\frac{x_2}{L} \end{bmatrix} \cdot u \tag{13}$$

considering now, without loss of generality, that the control variable is $u = 1 - q$. The new set of possible equilibrium points is

$$\Gamma = \left\{ x \in \mathbb{R}^3 \middle/ x_1 = \frac{{x_2}^2}{RE} \ \text{ e } \ x_3 = 0 \right\}. \tag{14}$$

Note that, despite the order increase in the state space model, the dimension of Γ remains the same. The switching surfaces of the sliding mode controller was designed considering this higher order model in a previous work [9], which resulted in the following controller,

$$u(x) = \begin{cases} 0 & \text{if } \sigma(x) > 0 \textbf{ and } \rho(x) > 0 \\ 1 & \text{else.} \end{cases} \tag{15}$$

with the switching surfaces defined by

$$\sigma(x) = \kappa + \alpha x_2 - x_3 = 0 \tag{16}$$

$$\rho(x) = \gamma + \beta x_1 - x_2 = 0 \tag{17}$$

and the surfaces defining parameters set to $\kappa = 11.43$, $\alpha = -0.1143$, $\gamma = 50$ and $\beta = -25$.

Since this is not a PWM technique, a hysteresis band is added to the control law in order to guarantee that the frequency of switching remain within the limits established in Section III-B. The method for determining the value of this hysteresis band can be found in [8].

The phase plane trajectories of the system under these two control laws are depicted in Fig. 5 for a load transition from 40Ω to 200Ω at $t = 1ms$ and back to 40Ω at $t = 4ms$. The time evolution of the state variables can be seen in Fig. 6 and Fig. 7.

The settling time for the case of an increase in resistance is about $2ms$ for the linear controller and $1ms$ for the nonlinear one. In the case of a decrease in resistance it is approximately $1ms$ for both controller. The overshoot is about 30% of the nominal output voltage for the linear controller when load decreases and the undershoot is 25% when it increases. The sliding mode controller with washout filter shows a better performance, and gets lose to the optimal response. Fig.(5)b shows how the closed-loop trajectory under a load disturbance gets close to the natural trajectories ϕ_0 and ϕ_1. Despite this fact, the undershoot is also about 25% because of the high ripple in the full load operation. Although, when the load is reduced, the overshoot is about 24%, very close to optimal.

V. CONCLUSIONS

From the results obtained by simulation of the DC-DC boost converter, it can be seen that the qualitative behaviours of the closed-loop boost with the two different controllers are quite similar. The nonlinear controller shows a better overall performance with the advantage of being able to take the boost from the zero state and lead it to the nominal operating point in short time without the necessity of auxiliary devices. Although, none of the controllers could optimize the system response to a load disturbance to a performance better than that accomplished by following the natural trajectories. This

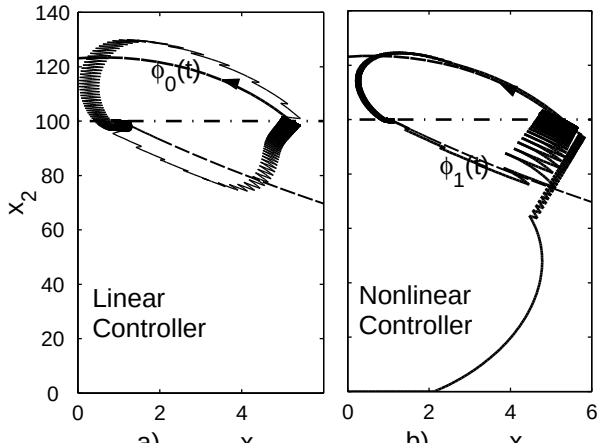

Fig. 5. System trajectories in the state space (x_1, x_2), for two different controllers. a) Linear PID controller. b) Nonlinear sliding mode controller.

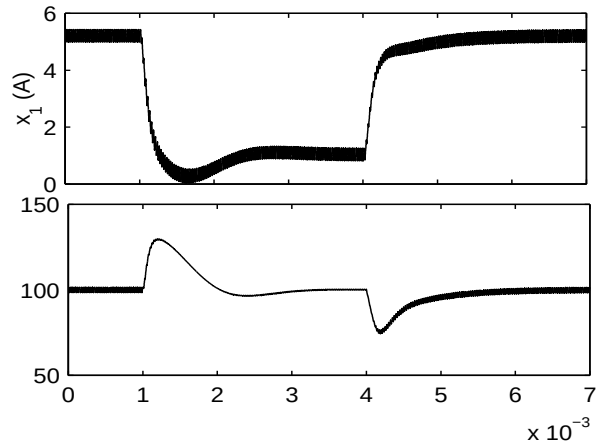

Fig. 6. Time response for the PID controller.

limitation is due to the intrinsic constraint on the control variable $0 \leq d \leq 1$. This indicates that the performance achieved with these two controllers can hardly be further improved, for any better controller would meet the saturation constraint.

The load disturbance rejection of the DC-DC boost converter is shown to depend on the inner structural characteristics of the system. The saturation of the control variable imposes a definitive limitation on the controller performance. To minimize the effect of load disturbances, the desired transient behaviour of the output voltage has to be considered in the design phase of the system.

Since most power electronic devices are based on switching, the saturation effects are always present. This suggests that the results presented in this paper could be extended to other converters.

REFERENCES

[1] J. G. Kassakian, M.F. Schlecht, and G. C. Verghese, *Principles of Power Electronics*, Addison-Wesley, Massachusetts, 1991.

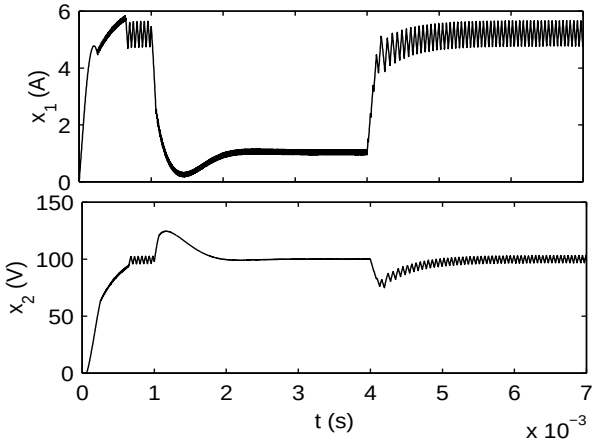

Fig. 7. Time response for the nonlinear controller (sliding mode controller).

[2] P. T. Krein, *Elements of Power Electronics*, Oxford University Press, New York, 1998.

[3] R. D. Middlebrook and S. Cúk, "A general unified approach to modelling switching-converter power stages," *PESC*, pp. 18–34, 1976.

[4] H. Sira-Ramírez, R. A. Perez-Moreno, R. Ortega, and M. Garcia-Esteban, "Passivity-based controllers for stabilization of dc-to-dc power converters," *Automatica*, vol. 33, no. 4, pp. 499–513, 1997.

[5] G. Escobar, R. Ortega, H. Sira-Ramírez, J-P. Vilain, and I. Zein, "An experimental comparission of several nonlinear controllers for power converters," *IEEE Control Systems*, vol. 19, no. 1, pp. 66–82, 1999.

[6] P. T. Krein, *Nonlinear Phenomena in Power Electronics: atractor, bifurcations, chaos and nonlinear control*, chapter 8: Nonlinear Control and Control of Chaos, pp. 353–370, Edited by Banerjee S. and G. Verghese, IEEE Press, 2001.

[7] A. S. Martins, E. V. Kassick, and I. Barbi, "Control strategy for the double-boost converter in continuous conduction mode applied to power factor correction," *PESC*, vol. 2, pp. 1066–1072, 1996.

[8] F. B. Cunha, "Análise e controle de sistemas de estrutura variável," Master thesis (in portuguese), PGEEL-UFSC, UFSC, June 2002.

[9] F. B. Cunha and D. J. Pagano, "Conversor cc-cc elevador de tensão controlado por modos deslizantes com auxílio de filtro "washout"," *XIV Congresso Brasileiro de Automática - CBA*, pp. 1638–1643, 2002.

[10] I. E. Colling, *Conversores CA-CC monofásicos e trifásicos com elevado fator de potência*, Doctoral thesis (in portuguese), PGEEL-UFSC, UFSC, December 2000.